SSRG International Journal of Electronics and Communication Engineering
ISSN: 2348-8549/ https://doi.org/10.14445/23488549/IJECE-V13I7P123

Volume 13 Issue 7, 323-334, July 2026

Original Article

IoT-Augmented Framework for Driver Behavior and Terrain Identification using ZnO-Based Nanoionic Memristor

Subrat Kumar Pradhan[1], Saswat Panda[1], Sujata Chakravarty[2], Chandra Sekhar Dash[1*]

[1]*Department of Electronics and Communication Engineering, Centurion University of Technology and Management, Odisha, Bhubaneswar, India.*
[2]*Department of Computer Science Engineering, Centurion University of Technology and Management, Odisha, Bhubaneswar, India.*

**Corresponding Author : chandu0071@gmail.com*

Received: 28 April 2026 Revised: 06 June 2026 Accepted: 17 June 2026 Published: 29 July 2026

Abstract *- This study presents an IoT-enabled memristor-based nano-ionic system with its ZnO device to detect the vehicle terrain variations. An ADXL335 accelerometer is utilized to show driving dynamics, capture real-time motion data, and senses three perpendicular movements along X, Y, and Z axes. Under changing conditions, the electrical behaviour of the proposed memristor model can be analyzed by applying the measured signals. With precise timing information, the sensor data can be acquired and even stored by employing an ESP32 microcontroller, and so accurate analyses can be observed at a later stage. During the observations, the acceleration and deceleration patterns are reflected by the X-axis, while the Y-axis indicates side-to-side motion, and vertical displacements are recorded by the Z-axis owing to surface unevenness. The collected data is stored on a microSD card and subsequently used to evaluate the memristor model performance. The bipolar resistive switching behaviour is demonstrated by the ZnO-based Memristor, which is caused by the migration of oxygen vacancies, enabling the transition between high resistance and low resistance states through SET and RESET operations. On this basis, for each axis, approximately 6000 data samples were recorded, and for a detailed study, 500 samples per axis were chosen as representative points. Consistent hysteresis in conduction behaviour is produced by distinct variation in resistance led by changes in terrain conditions, and the characteristic here provides an effective difference between uneven, smooth, and rough road surfaces. Moreover, the Memristor, with its nonvolatile Nature, can retain electrical values associated with specific terrains, and the findings suggest that the IoT-based vehicle monitoring systems can be effectively integrated with this approach, offering improved durability, data retention, and performance for advanced intelligent transport applications.*

Keywords *- Accelerometer Sensor, EV Monitoring, Filamentary Current, Nano Ionic Memristor, Resistive Switching, ZnO Conduction.*

1. Introduction

Intelligent Transportation Systems (ITS) are essential to improve vehicle safety and operational effectiveness in today's technological environment. In this context, the use of Internet of Things (IoT) technology has been prompted based on sensors to enable sophisticated monitoring and control systems in automobiles. The development of autonomous driving and driver-assistance technologies has benefited greatly from these developments. Accelerometers have become one of the most affordable and dependable sensors for analyzing driving patterns, identifying vehicle maneuvers, and evaluating the state of the road surface. They are ideal for contemporary applications due to their high sampling rate, low power consumption, and simplicity of integration with microcontrollers and IoT platforms. Additionally, the significance of connected vehicle technology in real-time data analytics has grown, allowing for ongoing monitoring of road conditions and driver behavior.

Theorized as the “missing” fourth fundamental circuit element in 1971 by Leon Chua, the Memristor was first physically fabricated by HP Labs in 2008 as a state-dependent resistive switching device [1, 2]. The analog resistive tuning feature of Memristor can be implemented to obtain clearer data on driving patterns and road surface monitoring. The continuous resistance modulation makes it ideal for real-time event detection and adaptive control loops. The Ag/ZnO/FTO heterostructure is a highly suitable platform for memristive and neuromorphic devices due to its intrinsic electrochemical and interfacial advantages. ZnO provides a wide bandgap [3], high defect tenability, and a stable oxide matrix that supports controlled oxygen vacancy and Ag^{+} ion migration, and it exhibits stable bipolar switching. Compared with conventional TiO_2-, HfO_2-, and ITO-based memristors reported by Tominov et al. [4], Ag/ZnO/FTO devices exhibit lower forming voltage, stronger filament controllability, and superior switching uniformity [5-8]. In this work, we have used the proposed fabricated device and MATLAB-based simulation model, which mimics the characteristics of the actual memristor device.

Table 1. Brief literature survey of related studies

Sl.No.	Author	Contribution	Reference
1	Jachimczyk et al.	Real-time data collection of driving style using a multi-axis accelerometer	[9]
2	Cervantes-Villanueva et al.	Vehicle maneuvering like Hard Braking, Rapid Acceleration, and Rash driving sensing. Road surface identification using the vibration Pattern from vertical axis data from the sensor.	[10]
3	Surblys et al.	Road type(Asphalt, Cobblestone, damaged road) identification from the vertical axis vibration pattern	[11]
4	Khaleghian et al. Ward et al.	Different terrains generate unique vibration patterns obtained from Accelerometer and implementing them into an intelligent transportation and monitoring system.	[12] [13]
5	Lee et al.	Framework utilises the smartphone's builtin Accelerometer and camera as the primary sensing element to detect and collect direct data.	[14]
6	Xu et al. Zhao, W. et al.	compared Accelerometer in smartphones and the embedded system-based sensor in the vehicle monitoring system	[15] [16]
7	Egaji et al.	Machine-Learning models, including Random Forest and k-Nearest Neighbours to identify various vibration patterns to identify road conditions.	[17]
8	Silva et al.	proposed a product "TripMD" to identify various recurring patterns from time-series Accelerometer data using the motif detection technique.	[18]
9	Strączkiewicz et al.	analyse continous sensor data stream collected through IoT infrastructure to identify driving patterns in real-time.	[19]
10	Joubert et.al. Phan et al.	Driver-state evaluation to detect drowsiness and monitoring behavioural patterns through Accelerometer.	[20] [21]
11	Qin et al.	IoT IoT-based multi-sensor approach using Accelerometer, gyroscope, and contextual variables to identify driving patterns, focusing on reliability and robustness	[22]
12	Tang et al.	Use the smartphone's built-in Accelerometer to capture motion signatures and identify the features to categorise transportation modes.	[23]
13	Du et al. Kotha et al.	Smartphone based sensor used to identify potholes and Road-Bumps from the data collected using Gaussian background feature extraction and the k-nearest neighbour classifier	[24] [25]
14	Ozoglu et al.	A CNN-based approach to classify potholes and manholes from vibration data collected from a smartphone.	[26]
15	Kim, Y. M. et al. Kusakunniran et al. Kim et al.	Automated data collection and CNN-based classification to identify different vibration patterns with respect to speed for the same defect on the road.	[27] [28] [29]
16	Meocci et al. Yu et al.	Vehicle parameter correction with respect to realtime data collected for roughness and road anomaly at variable speed.	[30] [31]
17	Zhang, Z. et al. Guerra et.al.	hybrid system using a smartphone and a multi-vehicle approach to estimate roughness indices at variable speed.	[32] [33]
18	Raslan et al.	Integrating multiple algorithms for pattern recognition in vibration data has emerged as a highly effective approach utilizing wavelet, time-domain, and spectrogram-based features to classify potholes, speed bumps, and pavement types	[34]
19	Surblys et al.	Comparative analyses indicate that CNNs, conventional classifiers, and hybrid techniques such as RMS/PSD combined with RF or CNN demonstrate strong robustness and deliver reliable performance even in noisy environments. Utilising	[35]

		crowdsourcing or large-scale studies is a smart approach to monitor the defects on road.	
20	Alam, M. Y. et al. Martinez-Ríos et al. Aleadelat et.al.	Accelerometer and GPS streams used to process the information using a clustering technique and produce accurate localized defects that match localised ground defects. Used vibration-based techniques and concluded that crowdsourcing provides a cost-effective mechanism to monitor large urban area quickly and accurately.	[36] [37] [38]

Further, it is evident that real-time based monitoring has the accelerometer-based terrain and driving pattern monitoring from scattered implementation towards a multimodal approach where coherent validation plays an important role. Many focus points have been identified, such as: (a) the need of pre-processing to pay for speed and increased vehicle dynamics, (b) lightweight Deep Learning to compensate for noisy vibrations, (c) crowdsourcing to meet the scale of coverage, (d) utilizing edge/cloud processing for real-time response. It can be concluded from the above study that the use of an accelerometer to monitor makes a system scientifically sound and operationally possible framework to implement for smart-city road maintenance, fleet deployment, and adaptive vehicle systems. In this work, for the first time, we have proposed the implementation of an IoT augmented nano ionic memristor model based on ZnO into terrain identification in vehicles.

2. Methodology

Recently, the transportation system is a crucial component of the developing society. Any kind of abnormality would result in disruption. The primary objective of this work is to monitor key operational parameters and assess the driver's behavior continuously in real-time. The obtained data is fed to a memristor model, and observe the output and identify the driver behavior from the modelled data.

To observe, collect, and analyze these objectives, a system was designed and developed around the ESP32 WROOM-32D microcontroller board. It has got sufficient computational capabilities to collect the data from various sensors and store them for our further applications.

In order to monitor the acceleration and braking behavior of the driver, the ADXL335 analog 3-axis accelerometer is used, while temporal correlation of events was achieved by integrating an RTC (Real-time clock) DS1307 for accurate timestamping of the recorded data. Continuous storage of data was facilitated by a micro-SD card module loaded with an 8GB memory card. The complete system hardware and configuration are clearly illustrated in Figure 1.

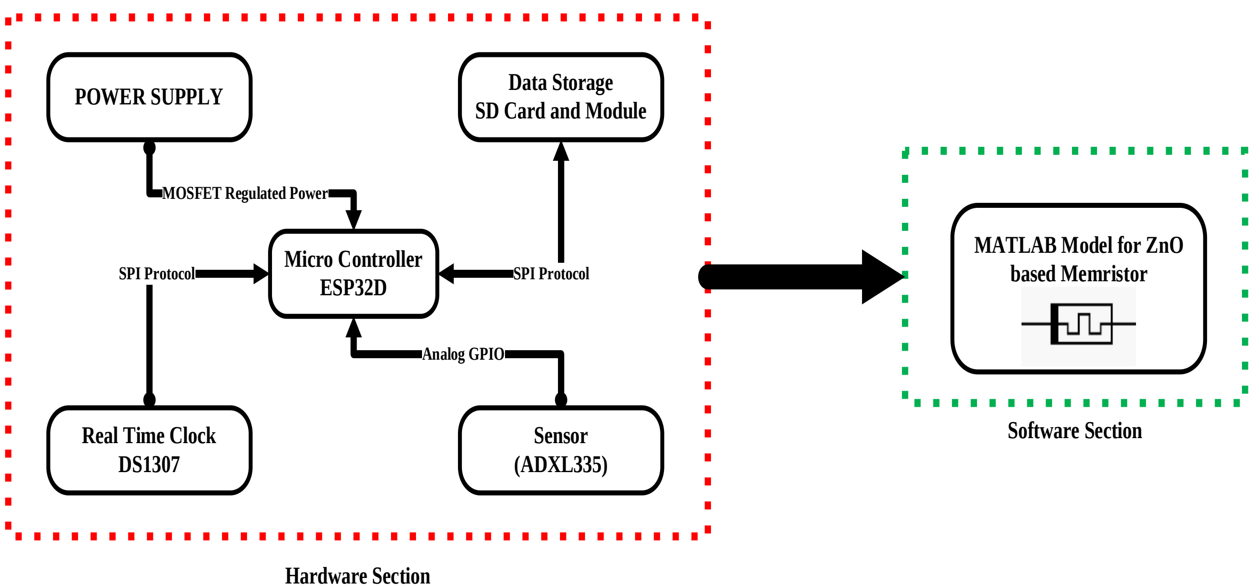

Fig. 1 Block diagram of the designed system illustrates the dependencies and role in the design

In the current analysis, the power supply unit is designed to provide stable, regulated power, which is vital for optimal system operation. It provides uninterrupted power to the ESP32 except when turned OFF intentionally while not in operation. The power is properly regulated to minimize any noise and power fluctuations to the Microcontroller, Sensor, and the peripheral Modules. The MOSFET-based regulator employed in the system enhances stability, measuring accuracy, and the corruption of data during storage. This makes the system suitable for continuous monitoring in all physical conditions. The ESP32 serves as the brain of the system, i.e., it processes the instructions strictly to serve the purpose. It is the primary unit responsible for the efficient operation of the integrated sensing and data logging functionalities within a low-power platform. Its architecture is dual-core, and extensive peripheral support makes it an efficient component for real-time data acquisition. It is equipped with built-in communication interfaces that facilitate the use of various sensors to the optimum capacity and enables future upgradation and integration.

In this regard, the ADXL335 triaxial accelerometer sensor is the core sensing component for the detection of acceleration, braking, and lateral movements. The variation in sensor reading corresponds to the change in velocity of the vehicle and the change in lateral direction. The data captured can be interpreted based on polarity, i.e., a positive value represents acceleration, while a negative value indicates braking. The data acquired along the 3 orthogonal axes represent: x-axis records the longitudinal motion (acceleration and braking), y-axis records the Lateral movement (Left and Right turning), and z-axis records the vertical motions (humps and bumps), surface irregularities in the road. Temporal correlation of sensor data is ensured by using an RTC module (DS1307) in the system. The RTC operates independently as it gets its power through an external battery, which enables it to maintain precise date and time even when the vehicle is in a power-down state. Whenever the ESP32 microcontroller is powered on, the system initializes and synchronizes with the RTC, and after which all the sensor data is time-stamped and recorded in a proper and systematic process. This enables chronological reconstruction during analysis.

Moreover, the data read from the sensor is time-stamped and stored on an SD card via an SD card module. This is an important component and plays a vital role in the monitoring system, providing a reliable, nonvolatile data storage medium which can be used for future references and analysis. The SD card module is connected to the ESP32 via the SPI communication protocol to ensure a stable and reliable method to store the data. Incorporating an SD card makes it easy and reliable to store large volumes of data efficiently, even though the system is offline, i.e., not connected to the network. The stored data set supports analysis of driver behavior, terrain analysis, and the development of future enhancements. Overall, the SD card subsystem enables reliability, scalability, and practicality in field applications. This data is stimulated to the memristor model, and characteristics are observed.

The designed circuit, along with ADXL335, was mounted on a two-wheeler. The vehicle was driven on a blacktop road where the road surface was having sections that were under maintenance, this was chosen to obtain the reading for smooth road and rough road. The sensor recorded parameters like acceleration, braking, left turn, right turn, smooth road and rough road. The test ride was conducted for about 10 minutes that accumulated approximately 6000 readings in each axis. The readings were identified through the time stamp (the pinion rider on the vehicle was noting down the time of event that would help in locating the readings from the raw data). The raw data was then fed into the model to obtain the corresponding memristance values for this work. These segregated readings (~500) were plotted, for ease identifying the differences in plot, the data points were further shortlisted.

3. Results and Discussion

3.1. Memristor Modelling

The Ag/ZnO/FTO memristive device exhibits bipolar resistive switching arising from the coupled effects of interfacial charge injection and conductive filament evolution inside the ZnO layer [3-5]. When a voltage is applied to the Ag top electrode with the FTO bottom electrode grounded, the electric field across the ZnO film controls both electronic transport and ionic migration. As observed in the experimental I-V characteristics in Figure 2, the device shows a hybrid conduction behavior in which interface-limited transport dominates in the High-Resistance State (HRS), while filamentary conduction governs the Low-Resistance State (LRS). At low bias in the HRS, the current is governed by Ohmic conduction followed by Schottky emission at the Ag/ZnO interface and Poole-Frenkel (PF) or trap-controlled Space Charge Limited Conduction (SCLC) inside the ZnO bulk [8]. The Schottky current density is given by

$$J_S = A^* T^2 \exp\left(-\frac{q\phi_B - \beta_S\sqrt{E}}{kT}\right) \tag{1}$$

where J_S is the current density, E is the electric field, A^* is the Richardson constant originates from thermionic emission theory and represents the material-specific factor in the current density equation. The term A^*T^2 represents the carrier supply function at temperature T. k is the Boltzmann's constant, and q represents the charge of an electron. β_S is the interface effect (Schottky barrier lowering coefficient) [3, 4]. The experimental device shows rectifying behaviour consistent with Schottky at Ag/ZnO.

$$J_{PF} \propto E e^{-\frac{q\phi_t - \beta_{PF}\sqrt{E}}{kT}} \tag{2}$$

where J_{PF} is the current density, ϕ_t is the trap depth energy level (eV) for PF and β_{PF} is the PF barrier-lowering coefficient has the same origin as Schottky lowering, but it applies to bulk trap states. A linear fit indicates Schottky as well as PF, but the test electrode changes (Schottky is electrode-limited, and PF is bulk-limited). $x(t)$ is the dynamical state of the memristor and modelling with $x(t)$ captures hysteresis [5].

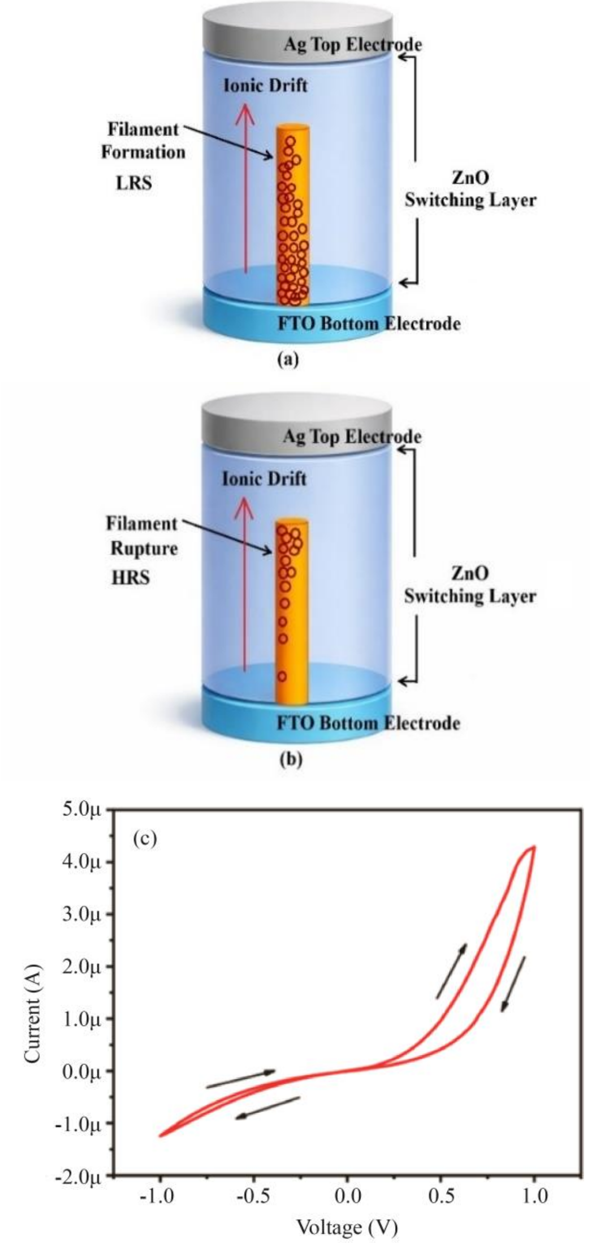

Fig. 2 Enabling, (a) Reliable filament formation, and (b) Filament rupture, (c) I-V characteristics of Ag/ZnO/FTO (Reprinted with permission from Ref. [3, 8]).

When the applied electric field exceeds a threshold, Ag^+ ions and oxygen vacancies migrate and accumulate, initiating the growth of a metallic filament inside ZnO. The internal state of the Memristor is described by a normalized variable x ($0 \leq x \leq 1$), representing the fractional length of the filament. The evolution of x is governed by field-driven ionic drift and thermally activated rupture, which can be mentioned as

$$\frac{dx}{dt} = \mu E\, f(x) - \Gamma e^{-E_a/kT} g\,(x, I, T) \tag{3}$$

where μ is ionic mobility, E_a is the rupture activation energy, Γ is the rupture prefactor, and $f(x)$, $g(x)$ are window functions that confine filament dynamics near the electrodes. Before complete filament formation, electron tunnelling occurs between the filament tip and the counter electrode. This tunnelling current is given by

$$I_{tun} = I_0 \exp(-\alpha d) \tag{4}$$

where α is the attenuation coefficient, and d is the tunnelling gap width. Once the filament bridges the electrodes, current flows mainly through the metallic channel and follows Ohmic conduction.

$$I_f = {}^{V}/_{R_{on}} \tag{5}$$

The total device current is therefore the sum of bulk ZnO conduction, tunnelling current, and filamentary current.

$$I = I_{bulk} + I_f + I_{tun} \tag{6}$$

where I_{bulk} consists of Schottky, PF, and SCLC components [6] and is the current flowing through the ZnO matrix (non-filamentary path). Additionally, it represents all conduction mechanisms that occur before a metallic filament bridges the device. Since conduction occurs through two parallel paths, the insulating ZnO matrix and the metallic filament, the effective memristance is governed by the internal state variable x, and it can be defined as

$$M(x) = xR_{on} + (1 - x)R_{off} \tag{7}$$

where R_{on} is the resistance of the conductive filament (LRS) and R_{off} is the resistance of the ZnO bulk (HRS).

3.2. Proposed Model

Contemporary vehicles use sensors to monitor driving behavior, road conditions, vibrations, speed, and location, with this study focusing on accelerometer data combined with memristor-based memristive properties for enhanced analysis purposes. Using accelerometer data and the changes in memristance values of this system, the main purpose is to identify, record, and compare different vehicle events, which provides proper road condition analyses and vehicle motion understanding. Moreover, the main controller is the microcontroller ESP32, is used by the system, which is connected to an accelerometer ADXL335. Further, the system uses a DS1307 Real-Time Clock (RTC) and an SD card module in order to store the data.

The Accelerometer is mounted in a specific position where the x-axis points in the forward direction of the vehicle and the z-axis points vertically upward, where the acceleration and braking are measured by the x-axis, and the left-right turns, which are the side movements, are measured by the y-axis. Additionally, the vertical movements, such as bumps, potholes, and uneven road surfaces, are captured by the z-axis. The vibration data from all three axes is processed and given to a memristor model to study changes in memristance. The analysis regarding the patterns and labels of different events is then made by these memristance variations, and thus makes the model useful for road defects detection system.

As illustrated in Figure 3, the working process of the system starts by powering on the ESP32 microcontroller, and in the beginning, it initializes all the connected modules. Further, the system configuration to ensure proper performance, storing, and time tracking, includes the initialization of ADXL335, SD card, and RTC, respectively. After that, the ESP32 tries to connect to Wi-Fi to get the current date and time from an online source. If the Wi-Fi connection fails, the system uses the DS1307 RTC through the I2C communication bus as a backup to obtain the time.

When the correct time is established, the analog data from the Accelerometer, which usually falls in the range of 0 to 4095 in digital form, continuously read by the ESP32. In this context, before starting the normal operation when the vehicle is stationary, the sensor is calibrated with the readings, where the output voltage is adjusted between +5V and 5V, with 0V taken as the reference point. Each reading is then given a timestamp and saved in a CSV file named “accel_log.csv” on the SD card for future analysis. This data acquisition and storage process persists uninterrupted as long as the system remains powered.

3.2.1. Working Principle of the Model

The power supply is connected to the ESP32 through the “VIN” and “GND” pins, that supplies power to the entire system. All the components used in the prototype run in 3.3V. So, the AMS1117 regulator of the ESP32 Module converts 5V to 3.3V, which is used throughout. This power is shared to all the remaining sensors and modules, like the SD Card Module, RTC, and ADXL335. The SD Card module is connected to the SPI bus via the GPIO pins 23, 19, 18, and 5 (MOSI, MISO, SCK, and CS, respectively). The Accelerometer (ADXL335) is connected to GPIO pins 34, 35, 32 (x-axis, y-axis, and z-axis, respectively). The prototype is placed or installed on the vehicle such that the x- axis captures the forward and braking motion, the y-axis captures the lateral movement, and the z-axis captures the vertical motion. In this context, the RTC module utilizes the I2C protocol to communicate accurate temporal information so that the data stored in the SD card has proper temporal correlation is achieved. It is connected to the GPIO pins 21 and 22(SDA and SCL) respectively. This module has a built-in battery such that the RTC module maintains the proper time even if the system is powered off. The complete connection diagram is demonstrated in Figure 4.

Graphical representation of the data obtained from the Accelerometer is demonstrated in Figure 5, where ‘P1’ in plot 5(a) represents vehicles at constant motion. When acceleration is applied to the vehicle, the ADXL335 responds as highlighted at ‘Q1,’ and the corresponding memristor response is shown in Figure 5(c) at ‘P2’ and ‘Q2’ as obtained from the model.

Considering the instances when the brake is applied to the moving vehicle, it is demonstrated in plot 5(b), where we can observe that at ‘R1’ the vehicle was in constant motion and the brake was applied, which is observed at ‘S1’ in the plot. The response of the Memristor can be seen in plot 5(d), highlighted as ‘R2’ and ‘S2’.

Furthermore, Figure 5 demonstrates the dynamic transformation of vehicular motion signals into resistive states of the Ag/ZnO/FTO memristor. When acceleration increases, the applied voltage rises, leading to a larger electric field across the ZnO switching layer. This field enhances oxygen vacancy migration and Ag filament nucleation inside the ZnO matrix [39]. The conductive filament fraction represented by the internal state variable (x(t) increases respectively. The memristance relation, which is mentioned earlier in the Equation (7), represents the accumulation of charge $q(t) = \int i(t)$ During acceleration, thereby continuously decreases the memristance [40]. This is observed in Figure 5(c), where it is evident that the memristance decreases as the acceleration voltage increases. Physically, this corresponds to the SET process, in which Ag ions drift from the top electrode and form conductive filaments in ZnO, turning the device into a Low Resistance State (LRS). The progressive thickening of the filament is a result of a decrease in memristance as acceleration increases, rather than abrupt switching instead. The vehicle dynamics are encoded into the analog memory, which is very much desired for such IoT-based signal encoding. The Memristor thus stores the acceleration history as a continuous resistance value. In contrast, Figure 5(b) shows the voltage profile during braking. Weakening of the electric field inside the ZnO results in an increase in memristance, which takes place as an outcome of the braking event, which reduces the voltage polarity and value across the Memristor. The AG filaments are responsible for conduction rupture because of this change in polarity and magnitude of voltage [41]. Consequently, the internal state variable x(t)decreases, leading to an increase in memristance, as shown in Figure 5(d). This is the RESET process, where the device transitions from LRS toward the High Resistance State (HRS). The increase in memristance takes place gradually as the conductive path ruptures in a gradual manner. This gradual RESET is governed by charge depletion in the device and thermal-assisted diffusion of Ag ions back into the electrode. Hence, it is clearly evident that the level of braking (i.e., rapid braking and soft braking) is encoded as an increase of memristance magnitude.

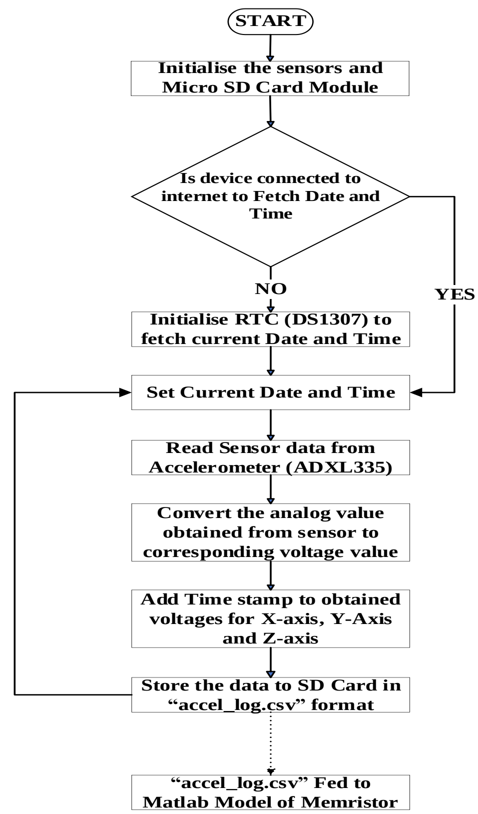

Fig. 3 Operation flow of the prototype

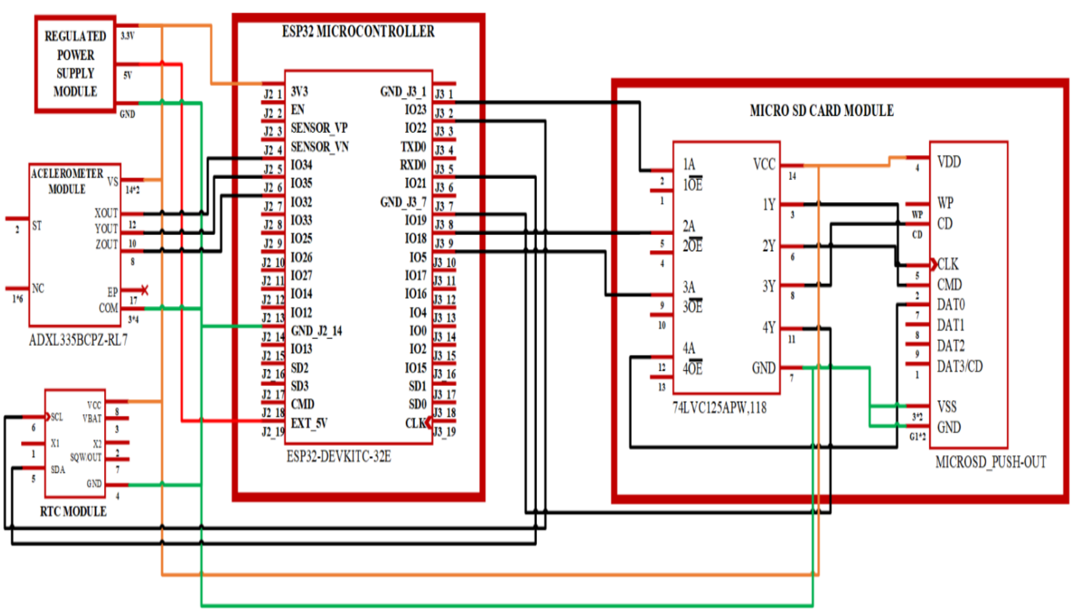

Fig. 4 Circuit connection diagram for hardware implementation

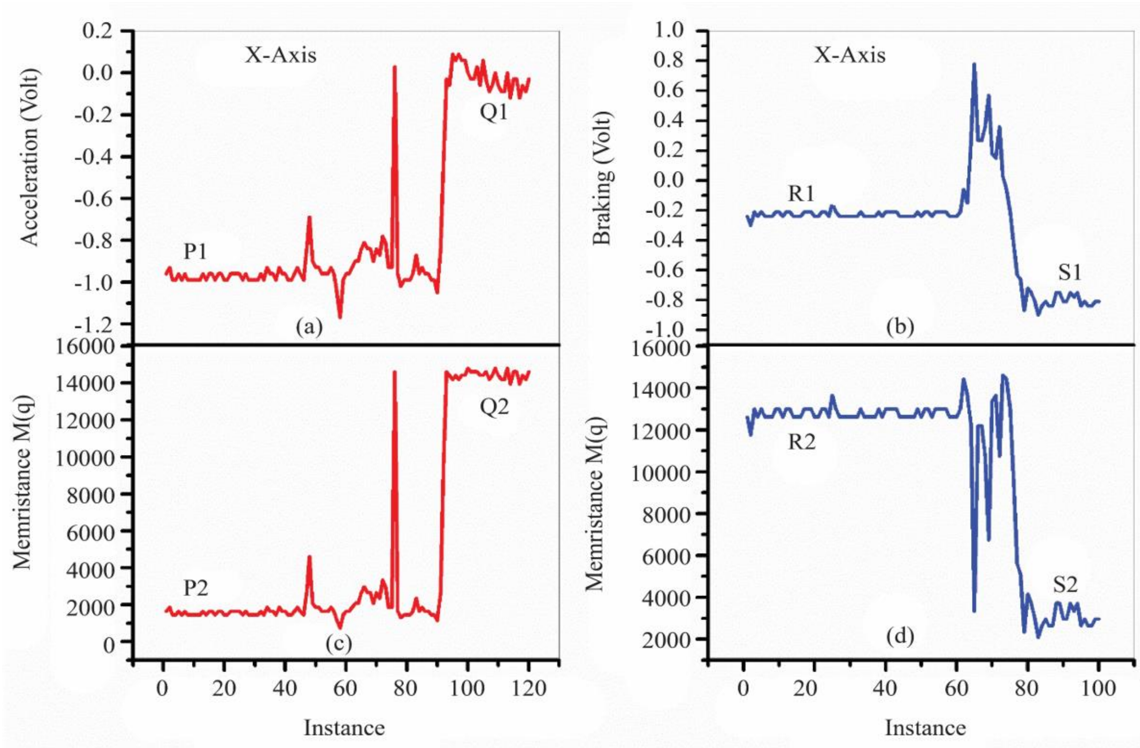

Fig. 5 Shows the X-axis information where (a) Acceleration, (b) Braking, (c) Memristor response to Acceleration voltages obtained from ADXL335, (d) Memristor response to Braking voltages obtained from ADXL335.

Figure 6 is focused on lateral motion of vehicle, where 6(a) shows the response of the Accelerometer as the vehicle takes a left turn, so the voltage level is reducing towards negative voltage highlighted at 'P3,' and the effect on memristance is shown in plot 6(c) at 'P4'. 6(b) represents the lateral motion to the Right, where we can observe that the voltage is increasing to a positive voltage at 'Q3'. And the respective response is seen at plot 6(d) at 'Q4'.

Additionally, Figure 6 illustrates how steering direction influences the electrical and memristive behavior of the Ag/ZnO/FTO device. Figure 6(a) and 6(b) show voltage signals corresponding to Left and right steering during acceleration. Steering induces asymmetric inertial forces on the vehicle, resulting in distinct voltage waveforms applied to the Memristor. These voltage asymmetries generate different current and charge flow patterns in the device. Since memristance depends on cumulative charge q(t), even small differences in voltage waveform shape led to significant divergence in memristance evolution. Figure 6(c) and 6(d) show that left-turn and right-turn motions result in distinct memristance trajectories. From a physical standpoint, the asymmetric voltage signals alter the electric field distribution across the ZnO film, leading to nonuniform Ag filament growth. During a left turn, the higher effective voltage produces stronger vacancy drift and filament reinforcement, resulting in a faster drop in memristance. During the right turn, the comparatively weaker field produces slower filament growth, leading to a higher retained memristance [42].

This asymmetry allows the Memristor to encode direction-dependent vehicular behavior. The Memristor thus acts not merely as a resistor but as a direction-sensitive element, storing whether the vehicle is turning left or right through its resistance state [43]. Importantly, this behavior is consistent with the bipolar resistive switching Nature of Ag/ZnO/FTO devices. The direction and magnitude of voltage dictate the SET strength and hence the degree of filament formation. This makes memristance a powerful feature for steering-based pattern recognition in embedded vehicle monitoring systems. Figure 7(a) demonstrates the vibration experienced by the vehicle, and when travelling on a rumbly road, so it happens to be in the negative voltage axis. Whereas Figure 7(b) demonstrates vibrations on a comparatively smooth road, so the obtained data from the Accelerometer is on the positive voltage axis. Moreover, Figure 7 highlights the ability of the Ag/ZnO/FTO memristor to discriminate road conditions based on voltage fluctuations. Rough roads generate highly irregular and high-frequency voltage variations due to mechanical vibrations, whereas smooth roads produce more stable voltage signals. In Figure 7(a), the rough road voltage shows rapid oscillations, which translate into fluctuating current and charge injection into the Memristor [44]. This causes repeated partial SET and RESET events at the nanoscale, resulting in a noisy but elevated memristance profile in Figure 7(c). The frequent disruption of conductive filaments prevents the device from reaching a stable LRS, keeping memristance relatively high. In contrast, Figure 7(b) (smooth road) provides a steady voltage that enables stable filament growth. As a result, Figure 7(d) shows a smoother and lower memristance curve. This indicates a well-formed conductive path and reduced stochasticity in filament dynamics. Thus, the Memristor effectively acts as a road-condition sensor, where rough terrain corresponds to high, noisy memristance and smooth terrain corresponds to low, stable memristance [44]. This is directly linked to ZnO's sensitivity to electric field and thermal fluctuations affecting Ag filament stability.

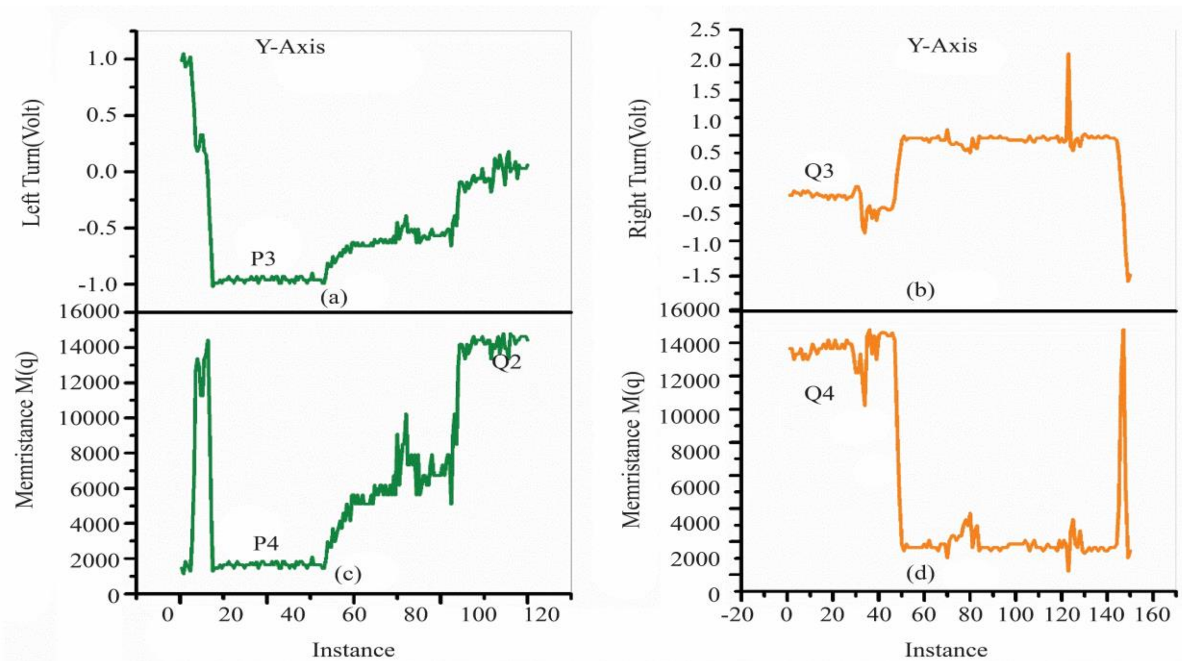

Fig. 6 Shows the response of the Accelerometer as the vehicle experiences the lateral motion, i.e., steering left and steering right. (a) Indicates the accelerometer response as the vehicle steers left, (b) Indicates the accelerometer response as the vehicle steers Right, (c) Left-turn motions result in distinct memristance trajectories, and (d) Right-turn motions result in distinct memristance trajectories.

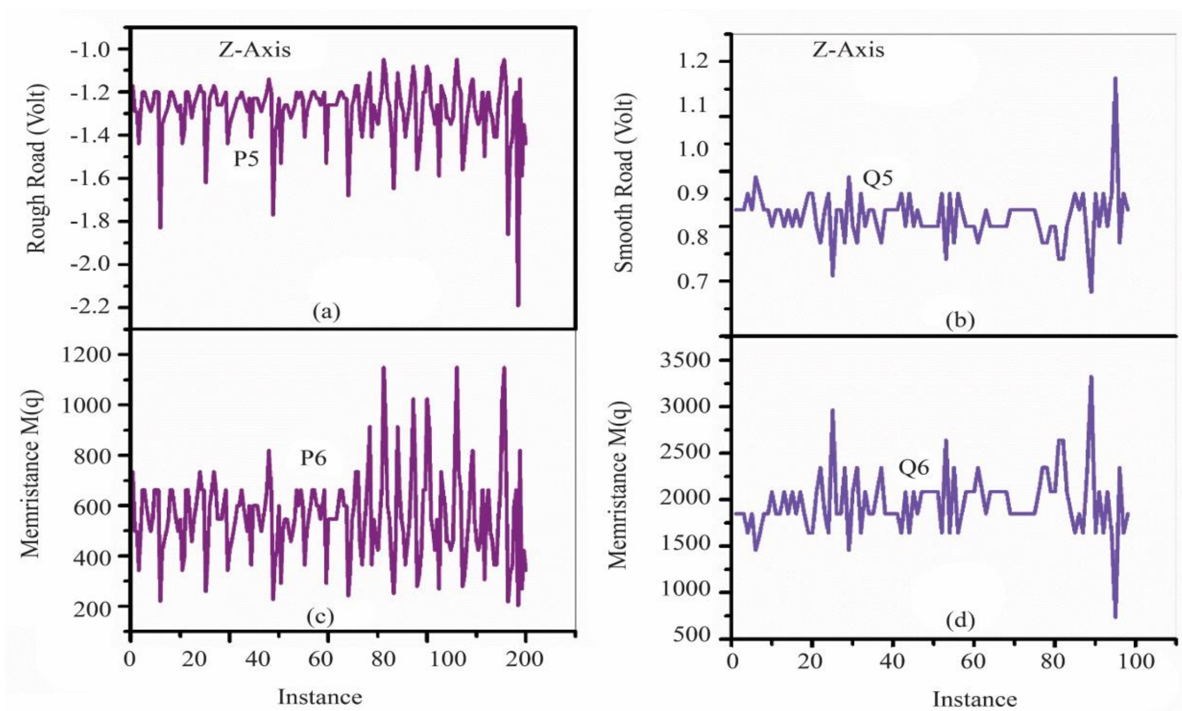

Fig. 7 Demonstrates the effect of the terrain on which the vehicle is moving, (a) Shows the sensor response of a vehicle moving on a rough road, (b) Demonstrates the sensor behavior when the vehicle is on smooth terrain, (c) and (d) Show the response of the memristor to the corresponding terrain.

4. Conclusion

This article presents a successful real-time IoT application for driver behavior monitoring and terrain identification using a nano-ionic ZnO memristor model. An accelerometer collects real-time data, which is externally fed into the model to obtain memristor responses. These responses strongly correlate with accelerometer-derived inputs across all axes, showing distinct resistive modulation corresponding to acceleration, braking, steering, and varying road conditions. Acceleration and retardation (Braking) exhibit voltage changes which are abrupt and sharp in Nature, which generate a significantly visible change in conductance, confirming that the Memristor exhibits stable SET and RESET operations. Left and Right steering, i.e., lateral movements, are normally gradual operations which are clearly visible through the slow variation in memristance. This clearly helps us identify the lateral movement in the Y-axis. Rough road conditions generate higher fluctuation density and frequent state transitions, while smooth surfaces exhibit stable, low variance conductance behavior. The clear separation between high and low memristance states allows reliable classification of driving events and terrain types. Moreover, the nonvolatile Nature of the ZnO nano-ionic memristor ensures retention of these dynamic signatures, supporting accurate post-analysis. This approach highlights a greater opportunity for real-time application in vehicles where terrain detection and driver behavior analysis is a key factors for future road safety. This system can be further enhanced to meet predefined parameters related to the prediction of road risk and optimizing the vehicle parameters in order to respond to the real-time road conditions. This can be a significant key to support autonomous vehicle driving systems through efficient data processing and neuromorphic computing capabilities.

Acknowledgements

All the work presented in this paper has been carried out in the laboratories of Centurion University of Technology and Management, Bhubaneswar.

Conflict of Interest

The authors declare no conflicting interests.

Funding Declaration

No external funding was provided for the completion of this research. The authors independently managed the research process, including conceptualization, methodology, data analysis, and the preparation of the final manuscript.

Data Availability Declaration

All relevant data supporting the findings of this study are presented within the manuscript. Any additional information or materials can be obtained from the corresponding author upon reasonable request.

References

[1] L. Chua, "Memristor-The Missing Circuit Element," *IEEE Transactions on Circuit Theory*, vol. 18, no. 5, pp. 507-519, 1971. [CrossRef] [Google Scholar] [Publisher Link]

[2] Dmitri B. Strukov et al., "The Missing Memristor Found," *Nature*, vol. 453, pp. 80-83, 2008. [CrossRef] [Google Scholar] [Publisher Link]

[3] Subrat Kumar Pradhan et al., "IoT Augmented Metal Oxide Memristor-based Vehicle Monitoring System," *Journal of Materials Science: Materials in Electronics*, vol. 36, no. 25, 2025. [CrossRef] [Google Scholar] [Publisher Link]

[4] Roman V. Tominov et al., "Nanoscale-Resistive Switching in Forming-Free Zinc Oxide Memristive Structures," *Nanomaterials*, vol. 12, no. 3, pp. 1-17, 2022. [CrossRef] [Google Scholar] [Publisher Link]

[5] R. J. Gray, "*Development of a Low-Cost Zinc Oxide-based Material Hybrid Memristor*," Ph.D. Thesis, University of Hull, 2017. [Google Scholar]

[6] Fengpo Yan et al., "Schottky or Ohmic Metal-Semiconductor Contact: Influence on Photocatalytic Efficiency of Ag/ZnO and Pt/ZnO Model Systems," *ChemSusChem*, vol. 7, no. 1, pp. 101-104, 2014. [CrossRef] [Google Scholar] [Publisher Link]

[7] Ayesha Zaman, "*Modeling and Experimental Characterization of Memristor Devices for Neuromorphic Computing*," Ph.D. Thesis, University of Dayton, 2020. [Google Scholar]

[8] Saswat Panda, and Chandra Sekhar Dash, "Modelling of Temperature Dependent Conduction and Filament Dynamics in Ag/ZnO/FTO Memristor," *Journal of Ovonic Research*, vol. 21, no. 6, pp. 833-843, 2025. [CrossRef] [Google Scholar] [Publisher Link]

[9] Bartosz Jachimczyk et al., "IoT On-Board System for Driving Style Assessment," *Sensors*, vol. 18, no. 4, pp. 1-22, 2018. [CrossRef] [Google Scholar] [Publisher Link]

[10] Javier Cervantes-Villanueva et al., "Vehicle Maneuver Detection with Accelerometer-Based Classification," *Sensors*, vol. 16, no. 10, pp. 1-23, 2016. [CrossRef] [Google Scholar] [Publisher Link]

[11] Vytenis Surblys et al., "Accelerometer-Based Pavement Classification for Vehicle Dynamics Analysis Using Neural Networks," *Applied Sciences*, vol. 14, no. 21, pp. 1-26, 2024. [CrossRef] [Google Scholar] [Publisher Link]

[12] Seyedmeysam Khaleghian, and Saied Taheri, "Terrain Classification using Intelligent Tire," *Journal of Terramechanics*, vol. 71, pp. 15-24, 2017. [CrossRef] [Google Scholar] [Publisher Link]

[13] Chris C. Ward, and Karl Iagnemma, "Speed-Independent Vibration-based Terrain Classification for Passenger Vehicles," *Vehicle System Dynamics*, vol. 47, no. 9, pp. 1095-1113, 2009. [CrossRef] [Google Scholar] [Publisher Link]

[14] Taehee Lee, Chanjun Chun, and Seung-Ki Ryu, "Detection of Road-Surface Anomalies Using a Smartphone Camera and Accelerometer," *Sensors*, vol. 21, no. 2, pp. 1-17, 2021. [CrossRef] [Google Scholar] [Publisher Link]
[15] Yi Xu et al., "VIDAR-Based Road-Surface Pothole-Detection Method," *Sensors*, vol. 23, no. 17, pp. 1-19, 2023. [CrossRef] [Google Scholar] [Publisher Link]
[16] Wei Zhao et al., "Real-Time Vehicle Motion Detection and Motion Altering for Connected Vehicle: Algorithm Design and Practical Applications," *Sensors*, vol. 19, no. 19, pp. 1-23, 2019. [CrossRef] [Google Scholar] [Publisher Link]
[17] Oche Alexander Egaji et al., "Real-Time Machine Learning-based Approach for Pothole Detection," *Expert Systems with Applications*, vol. 184, 2021. [CrossRef] [Google Scholar] [Publisher Link]
[18] Maria Inês Silva, and Roberto Henriques, "TripMD: Driving Patterns Investigation via Motif Analysis," *Expert Systems with Applications*, vol. 184, 2021. [CrossRef] [Google Scholar] [Publisher Link]
[19] M. Strączkiewicz et al., "Automatic Car Driving Detection using Raw Accelerometry Data," *Physiological Measurement*, vol. 37, no. 10, 2016. [CrossRef] [Google Scholar] [Publisher Link]
[20] Johan W. Joubert, Dirk de Beer, and Nico de Koker, "Combining Accelerometer Data and Contextual Variables to Evaluate the Risk of Driver Behaviour," *Transportation Research Part F: Traffic Psychology and Behaviour*, vol. 41, pp. 80-96, 2016. [Google Scholar] [Publisher Link]
[21] Anh-Cang Phan, Thanh-Ngoan Trieu, and Thuong-Cang Phan, "Driver Drowsiness Detection and Smart Alerting using Deep Learning and IoT," *Internet Things*, vol. 22, 2023. [CrossRef] [Google Scholar] [Publisher Link]
[22] Yanjun Qin et al., "A Traffic Pattern Detection Algorithm based on Multimodal Sensors," *International Journal of Distributed Sensor Networks*, vol. 14, no. 10, pp. 1-16, 2018. [CrossRef] [Google Scholar] [Publisher Link]
[23] Qinrui Tang, and Hao Cheng, "Feature Pyramid biLSTM: Using Smartphone Sensors for Transportation Mode Detection," *Transportation Research Interdisciplinary Perspectives*, vol. 26, pp. 1-11, 2024. [CrossRef] [Google Scholar] [Publisher Link]
[24] Ronghua Du et al., "Abnormal Road Surface Recognition Based on Smartphone Acceleration Sensor," *Sensors*, vol. 20, no. 2, pp. 1-17, 2020. [CrossRef] [Google Scholar] [Publisher Link]
[25] Maheshwari Kotha et al., "PotSense: Pothole Detection on Indian Roads using Smartphone Sensors," *Proceedings of the 1st ACM Workshop on Autonomous and Intelligent Mobile Systems*, pp. 1-6, 2020. [CrossRef] [Google Scholar] [Publisher Link]
[26] Furkan Ozoglu, and Türkay Gökgöz, "Detection of Road Potholes by Applying Convolutional Neural Network Method Based on Road Vibration Data," *Sensors*, vol. 23, no. 22, pp. 1-19, 2023. [CrossRef] [Google Scholar] [Publisher Link]
[27] Young-Mok Kim et al., "Review of Recent Automated Pothole-Detection Methods," *Applied Sciences*, vol. 12, no. 11, pp. 1-15, 2022. [CrossRef] [Google Scholar] [Publisher Link]
[28] Chao Wu et al., "An Automated Machine-Learning Approach for Road Pothole Detection Using Smartphone Sensor Data," *Sensors*, vol. 20, no. 19, pp. 1-23, 2020. [CrossRef] [Google Scholar] [Publisher Link]
[29] Gyulim Kim, and Seungku Kim, "A Road Defect Detection System using Smartphones," *Sensors*, vol. 24, no. 7, pp. 1-21, 2024. [CrossRef] [Google Scholar] [Publisher Link]
[30] Monica Meocci et al., "A Vibration-Based Methodology to Monitor Road Surface: A Process to Overcome the Speed Effect," *Sensors*, vol. 24, no. 3, pp. 1-15, 2024. [CrossRef] [Google Scholar] [Publisher Link]
[31] Qiqin Yu, Yihai Fang, and Richard Wix, "Pavement Roughness Index Estimation and Anomaly Detection using Smartphones," *Automation in Construction*, vol. 141, 2022. [CrossRef] [Google Scholar] [Publisher Link]
[32] Shohel Rana, and Asaduzzaman, "Vibration Based Pavement Roughness Monitoring System Using Vehicle Dynamics and Smartphone with Estimated Vehicle Parameters," *Results in Engineering*, vol. 12, pp. 1-16, 2021. [CrossRef] [Google Scholar] [Publisher Link]
[33] Kevin Guerra et al., "Pothole Detection and International Roughness Index (IRI) Calculation using ATVs for Road Monitoring," *Scientific Reports*, vol. 14, pp. 1-11, 2024. [CrossRef] [Google Scholar] [Publisher Link]
[34] E. Raslan et al., "Evaluation of Data Representation Techniques for Vibration-Based Road Surface Classification," *Scientific Reports*, vol. 14, pp. 1-20, 2024. [CrossRef] [Google Scholar] [Publisher Link]
[35] Sang-Kwon Lee et al., "Road Type Classification Using Deep Learning for Tire-Pavement Interaction Noise Data in Autonomous Driving Vehicle," *Applied Acoustics*, vol. 212, 2023. [CrossRef] [Google Scholar] [Publisher Link]
[36] Munshi Yusuf Alam et al., "Crowdsourcing from the True Crowd: Device, Vehicle, Road-Surface and Driving Independent Road Profiling from Smartphone Sensors," *Pervasive and Mobile Computing*, vol. 61, 2020. [CrossRef] [Google Scholar] [Publisher Link]
[37] Erick Axel Martinez-Ríos, Martin Rogelio Bustamante-Bello, and Luis Alejandro Arce-Sáenz, "Review of Road Surface Anomaly Detection and Classification Systems based on Vibration-Based Techniques," *Applied Sciences*, vol. 12, no. 19, pp. 1-26, 2022. [CrossRef] [Google Scholar] [Publisher Link]
[38] Waleed Aleadelat et al., "Evaluation of Pavement Roughness Using an Android-Based Smartphone," *Journal of Transportation Engineering, Part B: Pavements*, vol. 144, no. 3, 2018. [CrossRef] [Google Scholar] [Publisher Link]
[39] Tukaram D. Dongale et al., "Development of Ag/ZnO/FTO Thin Film Memristor using Aqueous Chemical Route," *Materials Science in Semiconductor Processing*, vol. 40, pp. 523-526, 2015. [CrossRef] [Google Scholar] [Publisher Link]

[40] Baker Mohammad et al., "State of the Art of Metal Oxide Memristor Devices," *Nanotechnology Reviews*, vol. 5, no. 3, 2016. [CrossRef] [Google Scholar] [Publisher Link]

[41] Fatih Gul, and Hasan Efeoglu, "ZnO and ZnO_{1-x} based Thin Film Memristors: The Effects of Oxygen Deficiency and Thickness in Resistive Switching Behavior," *Ceramics International*, vol. 43, no. 14, pp. 10770-10775, 2017. [CrossRef] [Google Scholar] [Publisher Link]

[42] Yong Huang et al., "Transition from Synaptic Simulation to Nonvolatile Resistive Switching Behavior based on an Ag/Ag:ZnO/Pt Memristor," *RSC Advances*, vol. 12, no. 52, pp. 33634-33640, 2022. [CrossRef] [Google Scholar] [Publisher Link]

[43] Alexander Vahl et al., "Concept and Modelling of Memsensors as Two Terminal Devices with Enhanced Capabilities in Neuromorphic Engineering," *Scientific Reports*, vol. 9, pp. 1-9, 2019. [CrossRef] [Google Scholar] [Publisher Link]

[44] Benjamin Kerr Barnes, and Kausik S. Das, "Resistance Switching and Memristive Hysteresis in Visible-Light-Activated Adsorbed ZnO Thin Films," *Scientific Reports*, vol. 8, pp. 1-10, 2018. [CrossRef] [Google Scholar] [Publisher Link]